FcgammaRIV is a mouse IgE receptor that resembles macrophage FcepsilonRI in humans and promotes IgE-induced lung inflammation.

David A. Mancardi, Bruno Iannascoli, Sylviane Hoos, Patrick England, Marc Daëron, Pierre Bruhns

FcγRIV is a mouse IgE receptor that resembles macrophage FcεRI in humans and promotes IgE-induced lung inflammation

David A. Mancardi,[1,2] Bruno Iannascoli,[1,2] Sylviane Hoos,[3,4] Patrick England,[3,4] Marc Daëron,[1,2] and Pierre Bruhns[1,2]

[1]Institut Pasteur, Département d'Immunologie, Unité d'Allergologie Moléculaire et Cellulaire, Paris, France. [2]INSERM, U760, Paris, France. [3]Institut Pasteur, Département de Biologie Structurale et Chimie, Plateforme de Biophysique des Macromolécules et de leurs Interactions, Paris, France. [4]CNRS, URA 2185, Paris, France.

FcγRIV is a recently identified mouse activating receptor for IgG2a and IgG2b that is expressed on monocytes, macrophages, and neutrophils; herein it is referred to as mFcγRIV. Although little is known about mFcγRIV, it has been proposed to be the mouse homolog of human FcγRIIIA (hFcγRIIIA) because of high sequence homology. Our work, however, has revealed what we believe to be new properties of mFcγRIV that endow this receptor with a previously unsuspected biological significance; we have shown that it is a low-affinity IgE receptor for all IgE allotypes. Although mFcγRIV functioned as a high-affinity IgG receptor, mFcγRIV-bound monomeric IgGs were readily displaced by IgE immune complexes. Engagement of mFcγRIV by IgE immune complexes induced bronchoalveolar and peritoneal macrophages to secrete cytokines, suggesting that mFcγRIV may be an equivalent of human FcεRI(αγ), which is expressed by macrophages and neutrophils and especially in atopic individuals, rather than an equivalent of hFcγRIIIA, which has no affinity for IgE. Using mice lacking 3 FcγRs and 2 FcεRs and expressing mFcγRIV only, we further demonstrated that mFcγRIV promotes IgE-induced lung inflammation. These data lead us to propose a mouse model of IgE-induced lung inflammation in which cooperation exists between mast cells and mFcγRIV-expressing lung cells. We therefore suggest that a similar cooperation may occur between mast cells and hFcεRI-expressing lung cells in human allergic asthma.

Introduction

A novel murine receptor for the Fc portion of mAbs (FcR) was recently cloned on the basis of a bioinformatics database search. This receptor is among the many FcR-like (FCRL) molecules identified in mammals, and it was first named murine FCRL3 (NCBI sequence BC027310) (1). FCRLs have no known ligand except murine FCRL3. As it was found to bind IgG, mouse FCRL3 was renamed mFcγRIV.

mFcγRIV binds mouse IgG2a and IgG2b with an intermediate affinity (equilibrium association constant [K_A] ≈ 2.9×10^7 M^{-1} and 1.7×10^7 M^{-1}, respectively; ref. 2). Two main types of FcRs can be distinguished on the basis of their affinity for immunoglobulins. Monomeric immunoglobulins can bind to high-affinity ($K_A \approx 10^8$–10^{10} M^{-1}) but not to low-affinity ($K_A \leq 10^6$ M^{-1}) receptors. As a consequence, a proportion of high-affinity receptors are occupied in vivo, whereas low-affinity receptors remain free, even though they are exposed to high concentrations of circulating immunoglobulins in vivo (3). Immune complexes (ICs) bind to low-affinity receptors with a high avidity. They also bind to high-affinity receptors. Both types of receptors signal when they are aggregated at the cell surface by mAbs and multivalent antigen (Ag). Rather than on the affinity of receptors, signals generated upon FcR aggregation depend on functional motifs contained in the intracellular domains of FcR subunits engaged in receptor aggregates.

mFcγRIV is an activating receptor (2). Like most activating FcRs, it associates with the common FcRγ subunit. FcRγ is a homodimer that contains 2 immunoreceptor tyrosine-based activation motifs (ITAM). The phosphorylation of FcR ITAMs by Src kinases initiates the constitution of an intracellular signaling complex, which activates an array of metabolic pathways leading to cell responses. FcRγ-dependent activation signals are amplified by FcRβ (4), another ITAM-containing subunit expressed in mast cells and basophils. mFcγRIV does not associate with FcRβ.

In order for mFcγRIV to be expressed at the cell membrane, it must associate with FcRγ (2). FcRγ indeed determines the membrane expression of multichain FcRs, i.e., mFcγRIV, human and murine high-affinity receptors for IgE (FcεRI) and IgG (FcγRI), and human and murine low-affinity receptors for IgG (FcγRIIIA) (5). FcRβ associates with multichain FcRs (6) expressed in mast cells and basophils (7). It is, however, mandatory for the expression of mFcεRI only (8, 9). hFcεRI can therefore be expressed with FcRβ [hFcεRI(αβγ)] in mast cells and basophils or without in monocytes, macrophages, and neutrophils [hFcεRI(αγ)], especially in atopic individuals. hFcεRI may therefore be expressed in 2 forms depending on the cell type and on the species. mFcγRIV is expressed in mouse monocytes, macrophages, and neutrophils.

mFcγRIV was recently reported to bind mouse IgE of the b (IgE^b) but not of the a (IgE^a) allotype (10). We show here that mFcγRIV is a low-affinity receptor for IgE irrespective of the 2 known allotypes (11, 12). FcγRIV does not exist in humans. On the basis of sequence

Nonstandard abbreviations used: Ag, antigen; BAL, bronchoalveolar lavage; BMMC, BM-derived mast cell; FcR, receptor for the Fc portion of mAbs; GaM, goat anti-mouse; IC, immune complex; IgE^a, IgE of the a allotype; IgE^b, IgE of the b allotype; i.n., intranasal(ly); ITAM, immunoreceptor tyrosine-based activation motif; K_A, equilibrium association constant; quintuple-KO mice, *mFcγRI/IIB/IIIA*$^{-/-}$ *mFcεRI*$^{-/-}$*mCD23*$^{-/-}$-deficient mice; SPR, surface plasmon resonance; TNP, 2,4,6-trinitrophenyl hapten.

Conflict of interest: The authors have declared that no conflict of interest exists.

Citation for this article: *J. Clin. Invest.* **118**:3738–3750 (2008). doi:10.1172/JCI36452.

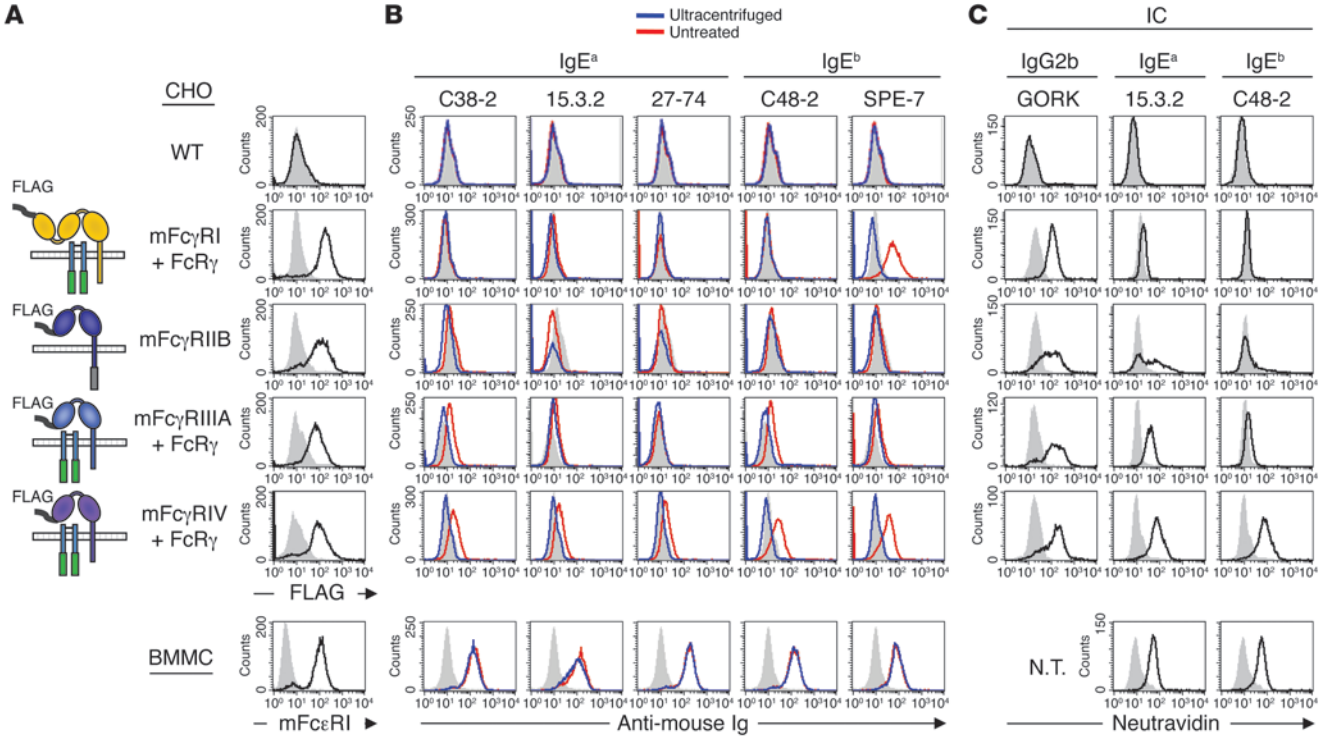

Figure 1

IgE ICs, but not monomeric IgE, bind to mFcγRIV. (**A**) Schematic representation of FLAG-tagged FcγR α chains associated or not with FcRγ expressed by transfectants. Green boxes represent ITAMs; the gray box represents an immunoreceptor tyrosine-based inhibition motif; the black stripe represents the FLAG-tag. Histograms show the binding of anti-FLAG mAb (black line) to FLAG-tagged FcγR on CHO transfectants and the binding of anti-mFcεRI mAb (black line) to mFcεRI on BMMCs or the binding of isotype control (solid gray). (**B**) Histograms show the binding of mouse IgE to FcγR$^+$ CHO and to BMMCs, using 50 μg/ml ultracentrifuged or nonultracentrifuged mouse IgE and 15 μg/ml FITC-conjugated F(ab′)$_2$ anti-mouse Ig. Solid gray histograms represent the binding of FITC-conjugated F(ab′)$_2$ anti-mouse Ig alone. The binding of SPE-7 to FcγRI was analyzed using 2 different lots of SPE-7 and each gave similar results. (**C**) Histograms show the binding of IgG2b ICs, IgE^a ICs, or IgE^b ICs to FcγR$^+$ CHO and to BMMCs as revealed by neutravidin staining. ICs were made using TNP_5-BSA-biotin and 15 μg/ml anti-TNP mAbs. Solid gray histograms show the binding of Ag alone as revealed by neutravidin staining. N.T., not tested. Data are representative of 2 (**B**) or 5 (**C**) independent experiments.

homology in extracellular domains, hFcγRIIIA was proposed to be the human homolog of mFcγRIV (1). We show that hFcγRIIIA has no detectable affinity for human IgE.

We also show that, in spite of having an intermediate affinity, mFcγRIV binds mouse IgG2a and IgG2b as monomers and functions as a high-affinity receptor. IgE ICs can, however, displace IgG2 from mFcγRIV. When aggregated by IgE ICs of both allotypes, mFcγRIV triggered Ca^{2+} responses in transfected cells and induced macrophage-like transformed cells and peritoneal macrophages to secrete TNF-α.

hFcεRI(αγ) has not only an affinity for IgE but also the same quaternary structure and a similar tissue distribution as mFcγRIV. The engagement of hFcεRI(αγ) was reported to activate monocytes (13) and neutrophils (14). We found that, when expressed by peritoneal macrophages from transgenic mice, hFcεRI(αγ) triggered similar TNF-α responses as endogenous mFcγRIV upon aggregation by IgE ICs. The expression of hFcεRI(αγ) is increased by monocytes, macrophages, and neutrophils of asthmatic patients. We found that mouse bronchoalveolar lavage (BAL) macrophages express neither mFcεRI nor mCD23 but express mFcγRIV, and they secreted TNF-α upon stimulation with IgE ICs. Finally, using mice deficient for *mFcγRI/IIB/IIIA*$^{-/-}$*mFcεRI*$^{-/-}$*mCD23*$^{-/-}$ (quintuple-KO), that only expressed mFcγRIV, we demonstrate that the in vivo engagement of mFcγRIV by IgE ICs synergizes with mediators released by IgE-activated mast cells to induce lung inflammation.

On the basis of these results, we propose that mFcγRIV is a low-affinity IgE receptor expressed by a subset of myeloid cells, and that, rather than hFcγRIIIA, hFcεRI(αγ) expressed by monocytes, macrophages, and neutrophils of atopic donors is the human equivalent of mFcγRIV. These properties endow mFcγRIV with what we believe to be novel physiopathological roles in murine models of allergic diseases and parasite infections.

Results

mFcγRIV, but not hFcγRIII, is a low-affinity IgE receptor. The binding of murine IgE was investigated on CHO transfectants expressing similar levels of FLAG-tagged murine FcγR (FcγR$^+$ CHO) (Figure 1A). High concentrations of 100,000 *g* ultracentrifuged monomeric IgE bound to mFcεRI-expressing mouse BM-derived mast cells (BMMCs) used as positive controls, but not detectably to FcγR$^+$ CHO (Figure 1B). Monomeric IgE of the 2 known allotypes, IgE^a and IgE^b, displayed the same binding properties. Nonultracentrifuged preparations of the same IgE, however, bound to mFcγRIV and mFcγRIIIA but not to mFcγRI or mFcγRIIB, except SPE-7, which bound also to mFcγRI. They bound in a manner similar to monomeric IgE binding to BMMCs (Figure 1B). Nonultracentri-

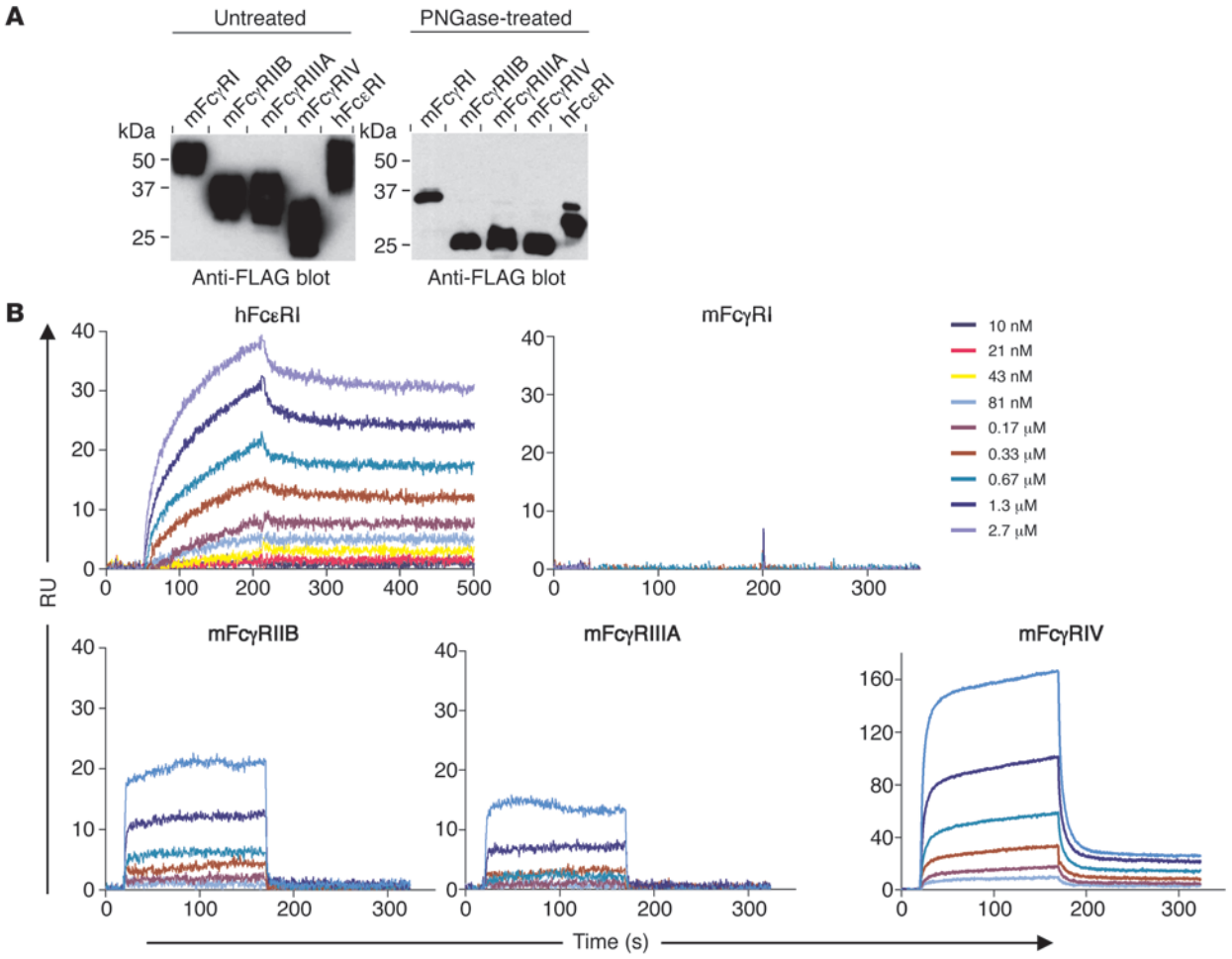

Figure 2
mFcγRI has a low affinity for IgE. (**A**) Untreated or PNGase-treated purified soluble extracellular domains of 3xFLAG-tagged FcR were submitted to SDS-PAGE and Western blotted using anti-FLAG–HRP mAbs. (**B**) Real-time SPR sensorgrams were generated by injecting the indicated concentrations of soluble monomeric IgE^b (C48-2^b) onto immobilized FcR ectodomains.

fuged IgE^b bound more efficiently to mFcγRIV than nonultracentrifuged IgE^a. These results indicate that nonultracentrifuged IgE preparations contained IgE aggregates that were removed upon ultracentrifugation, and that IgE aggregates but not monomeric IgE could bind to mFcγRIV. Untreated and ultracentrifuged IgE solutions were analyzed for homogeneity and aggregate content by dynamic light scattering (Supplemental Figure 1). Both untreated but not ultracentrifuged IgE^a and IgE^b contained aggregates, but IgE^b contained these in higher proportion than IgE^a. Noticeably, untreated IgE^b SPE-7 contained aggregates of bigger size than other IgE preparations. The higher proportion of aggregates among IgE^b than among IgE^a preparations may indeed explain their differential binding to mFcγRIV.

As mFcγRIV bound IgE aggregates, we investigated the binding of preformed IgE-Ag ICs and, as positive controls, of IgG2b ICs (2), to the same cells. IgG2b ICs bound comparably to mFcγRI, mFcγRIIB, mFcγRIIIA, and mFcγRIV. IgE ICs bound as efficiently as IgG2b ICs to mFcγRIV, less efficiently to mFcγRIIB and mFcγRIIIA, and not detectably to mFcγRI. mFcγRIIB and mFcγRIIIA were previously reported to behave as low-affinity IgE receptors (15). IgE ICs of the 2 allotypes bound comparably to mFcγRIV (Figure 1C). These results suggest that mFcγRIV has a low affinity for IgE.

To measure the affinity of mFcγRIV for IgE, FLAG-tagged extracellular domains of the 4 murine FcγRs and, as a positive control, of hFcεRI were produced in HEK293T cells. These molecules were N-glycosylated as demonstrated by SDS-PAGE analysis before and after peptide:N–glycosidase F treatment (Figure 2A). They were covalently immobilized onto activated dextran surfaces and used for surface plasmon resonance (SPR) analysis. IgE bound to mFcγRIV, mFcγRIIB, and mFcγRIIIA but not to mFcγRI. IgE bound to mFcγRIV with a K_A of approximately 2.6×10^5 M^{-1} (Tables 1 and 2). IgE bound with a 10-fold lower K_A to mFcγRIIB and mFcγRIIIA. It dissociated much faster from FcγRs than from hFcεRI (Figure 2B). The association rate constant (k_{on}) of IgE for mFcγRIV and for hFcεRI were of similar magnitudes, but the dissociation rate constant (k_{off}) of IgE for mFcγRIV was 250-fold higher (Table 1). As a consequence, IgE bound much more transiently to mFcγRIV ($t_{1/2} \approx 5$ seconds) than to hFcεRI ($t_{1/2} \approx 17$ minutes). Comparable kinetic parameters were obtained for 3 IgE^a and 2 IgE^b (Table 2).

Table 1
Kinetic parameters of soluble FcR ectodomains for IgE^b (C48-2)^A

	k_{on} ($M^{-1}s^{-1}$)	k_{off} (s^{-1})	$t_{1/2}$ (s)	K_A (M^{-1})	K_D (M)^B
mFcγRI	–/–	–/–	–/–	–/–	–/–
mFcγRIIB	n.m.	n.m.	n.m.	2.0×10^4	5.0×10^{-5}
mFcγRIIIA	n.m.	n.m.	n.m.	2.0×10^4	5.1×10^{-5}
mFcγRIV	2.60×10^4	0.1000	3	2.6×10^5	4.2×10^{-6}
hFcεRI	1.75×10^4	0.0003	1,000	5.9×10^7	1.7×10^{-8}

^{A}Data generated by injecting the concentrations of soluble monomeric IgE^b (C48-2^b) indicated in Figure 2B onto immobilized FcR ectodomains; $^B K_D$, equilibrium dissociation constant. –/–, no detectable binding; k_{off}, dissociation rate constant; k_{on}, association rate constant; n.m., not measurable.

Since hFcγRIIIA has been proposed to be the homolog of mFcγRIV, we investigated the binding of human IgE on another set of CHO transfectants expressing similar levels of FLAG-tagged hFcγRIIIA or hFcγRIIIB (Supplemental Figure 2A). The 2 known polymorphic variants of hFcγRIIIA (16) and the 3 known polymorphic variants of hFcγRIIIB (17, 18) were included. BMMCs from hFcεRI^{Tg} mice (19) were used as positive controls. High concentrations of monomeric human IgE bound to hFcεRI^{Tg} BMMCs but not to transfectants expressing hFcγRIIIA or hFcγRIIIB (Supplemental Figure 2B). The same concentrations of the same IgE failed to bind to hFcγRIII$^+$ CHO when in complex with F(ab′)$_2$ anti-human F(ab′)$_2$ (Supplemental Figure 2C). They also failed to bind to transfectants expressing hFcγRI, hFcγRIIA (H_{131} or R_{131} variants; ref. 20), hFcγRIIB, or hFcγRIIC (data not shown). These complexes, however, bound more avidly than monomers to hFcεRI^{Tg} BMMCs. Human IgE, therefore, do not bind to hFcγRIII. Supporting this observation, SPR analysis showed no measurable affinity of hFcγRIIIA (F_{176} or V_{176}) or hFcγRIIIB (NA1, NA2, or SH) for 3 human IgE (data not shown). These data altogether indicate that hFcγRIIIA is not the homolog of mFcγRIV as for their interactions with IgE.

IgE ICs displace monomeric IgG from mFcγRIV. mFcγRIV was described as having an intermediate affinity for mouse IgG2a and IgG2b. Although this affinity is at least 10-fold higher than that of murine low-affinity FcγR (2), IgG ICs bound similarly to mFcγRIV, to mFcγRIIB, and to mFcγRIIIA (Figure 1C). This affinity is 5-times lower than that of high-affinity mFcγRI (3), and we wondered whether monomeric IgG would bind to mFcγRIV. The same CHO transfectants that were used in Figure 1 were incubated with 100,000 *g* ultracentrifuged monomeric IgG1, IgG2a, or IgG2b. As expected, neither IgG1 nor IgG2b bound to mFcγRI, mFcγRIIB, or mFcγRIIIA, whereas IgG2a bound to mFcγRI but not to mFcγRIIB or mFcγRIIIA. Both IgG2a and IgG2b, but not IgG1, bound to mFcγRIV (Figure 3A). mFcγRIV, therefore, binds monomeric IgG2a and IgG2b, even though it has an intermediate affinity.

To investigate whether, when bound onto mFcγRIV and crosslinked, monomeric IgG2 can activate cells, we generated quintuple-KO mice. Such mice express mFcγRIV as their sole FcR. Thioglycolate-elicited peritoneal macrophages from these mice secreted comparable amounts of TNF-α upon challenge with F(ab′)$_2$ goat anti-mouse (GaM) when preincubated with monomeric IgG2a or IgG2b but not when preincubated with monomeric IgE^a or IgE^b (Figure 3B). mFcγRIV, therefore, functions as an activating high-affinity receptor for IgG2a and IgG2b.

mFcγRIV being also a low-affinity receptor for IgE, we wondered whether IgE ICs could bind to mFcγRIV in the presence of IgG. The binding of IgE ICs was reduced when mixed with a saturating concentration of IgG2a (Supplemental Figure 3A). IgG2a bound to mFcγRIV under these conditions, albeit slightly less than in the absence of IgE ICs (Supplemental Figure 3B). Likewise, the binding of IgE ICs was reduced but remained detectable when mFcγRIV$^+$ CHO were incubated with IgE ICs diluted 1:2 in normal mouse serum (Figure 3C). IgE^a and IgE^b behaved similarly in every condition. Therefore, IgE ICs and noncomplexed IgG2a compete with each other for binding to mFcγRIV.

We next investigated whether IgE ICs could bind to mFcγRIV when saturated by IgG. We found that IgE ICs could displace previously bound IgG2a (Supplemental Figure 3C) and bind to mFcγRIV (Supplemental Figure 3D). Likewise, we found that IgE ICs bound comparably to mFcγRIV$^+$ CHO, whether these were preincubated with normal mouse serum diluted 1:2 or not (Figure 3D). IgE of both allotypes behaved similarly. These data imply that IgG2a can dissociate from mFcγRIV. IgG2a and IgG2b indeed dissociated rapidly from mFcγRIV at 37°C ($3 \le t_{1/2} \le 10$ minutes) (Figure 3E). This observation is in keeping with the fast dissociation rates measured from SPR analysis (k_{off} [IgG2a] = 0.0631[±0.0145] s^{-1} and k_{off} [IgG2b] = 0.117[±0.011] s^{-1}; Figure 3F).

mFcγRIV engagement by IgE ICs activates macrophages. The aggregation of mFcγRIV by IgG2a ICs was reported to trigger a Ca^{2+} response in DT40 cells (2). Likewise, IgE ICs, but not monomeric IgE, induced an increase in the intracellular Ca^{2+} concentration of mFcγRIV$^+$ DT40 transfectants (Figure 4A). IgE of the 2 allotypes behaved similarly, except SPE-7, which triggered Ca^{2+} fluxes in the absence of Ag.

To determine whether mFcγRIV-dependent IgE-induced intracellular signals can induce biological responses, we first used the MH-S cell line. Because these cells express mFcγRI, mFcγRIIB/IIIA, and mFcγRIV but not mFcεRI or mCD23 (data not shown), they were preincubated with 2.4G2 F(ab′)$_2$ to block all IgE-binding receptors but mFcγRIV. Indeed, although intact 2.4G2 IgG bound to mFcγRIV$^+$ CHO, 2.4G2 F(ab′)$_2$ neither bound to mFcγRIV$^+$ CHO nor blocked the binding of IgE ICs. mAb 9G8 specifically recognized mFcγRIV and blocked IgE IC binding (Supplemental Figure 4, A and B). When crosslinked with F(ab′)$_2$ anti-Ig, 9G8 induced 2.4G2 F(ab′)$_2$–blocked MH-S cells to secrete TNF-α (Figure 4B). As previously reported, IFN-γ upregulated the expression of mFcγRIV (2), but not that of mCD23, on MH-S cells (Figure 4C). IFN-γ–treated, 2.4G2 F(ab′)$_2$–blocked MH-S cells secreted TNF-α when challenged with IgE ICs. They produced comparable amounts of TNF-α in response to IgE ICs or to IgG2b ICs (Figure 4D) and in

Table 2
Kinetic parameters of mFcγRIV ectodomains for mouse IgE^a and IgE^b ^{A}

	k_{on} ($M^{-1}s^{-1}$)	k_{off} (s^{-1})	$t_{1/2}$ (s)	K_A (M^{-1})	K_D (M)
IgE^a (27-74)	4.4×10^4	0.180	1.7	2.4×10^5	4.1×10^{-6}
IgE^a (15.3.2)	3.9×10^4	0.065	4.6	6.0×10^5	1.7×10^{-6}
IgE^a (C38-2)	2.6×10^4	0.180	1.5	1.4×10^5	7.1×10^{-6}
IgE^b (C48-2)	1.0×10^4	0.050	6.0	2.0×10^5	4.9×10^{-6}
IgE^b (SPE-7)	3.3×10^4	0.044	6.8	7.5×10^5	1.3×10^{-6}

^{A}Data generated by injecting soluble monomeric IgE^a and IgE^b onto immobilized mFcγRIV ectodomains.

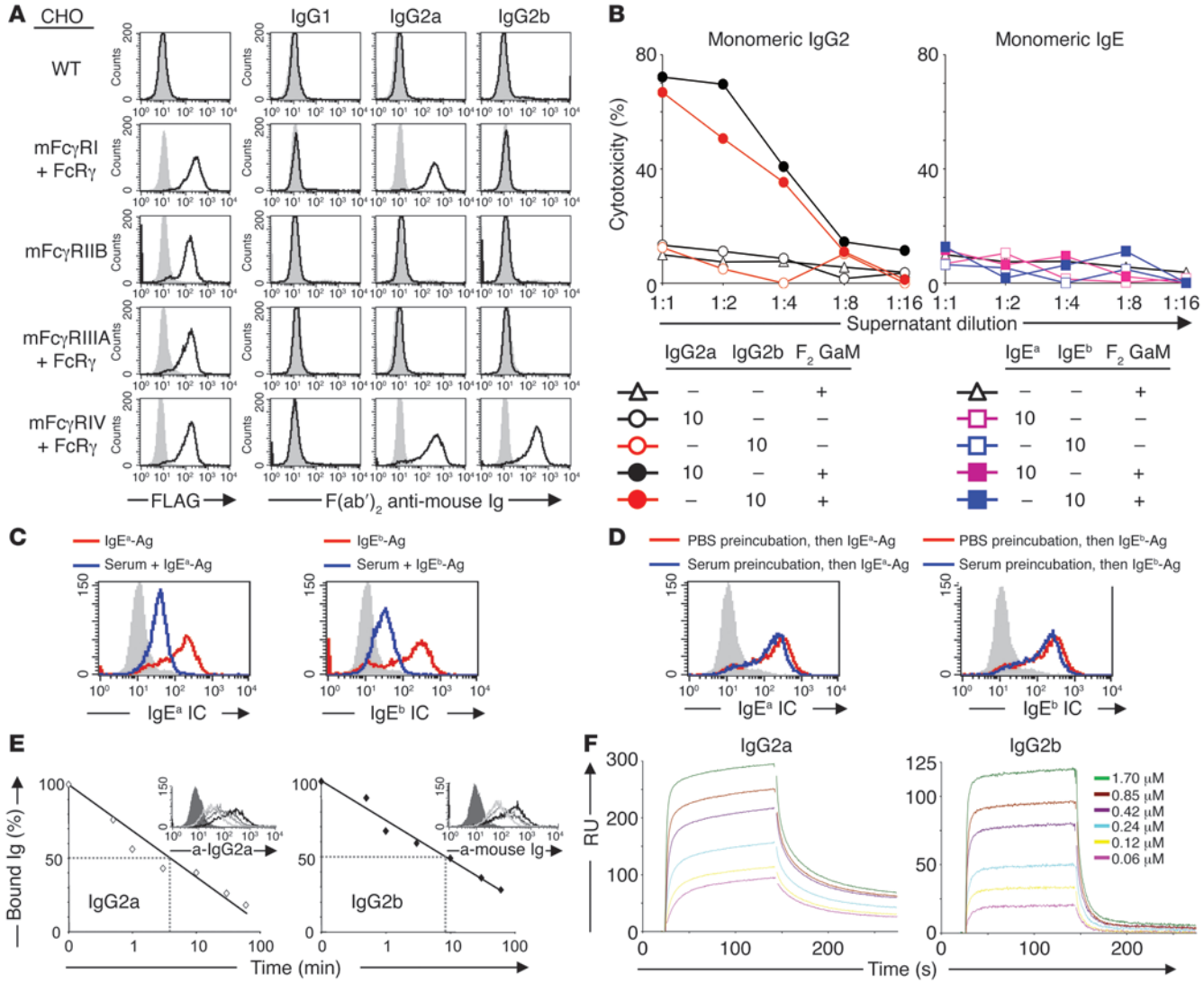

Figure 3

mFcγRIV is a high-affinity receptor for IgG2a/2b, but IgE ICs can bind to mFcγRIV in the presence of high IgG concentrations. (**A**) Histograms show the binding of monomeric mouse IgG1, IgG2a, or IgG2b (27–35) (10 μg/ml 100,000 *g* ultracentrifuged) to FcγR$^+$ CHO, revealed by FITC-conjugated F(ab′)$_2$ GaM. (**B**) Thioglycolate-elicited peritoneal macrophages from quintuple-KO mice were incubated with indicated concentrations of monomeric mouse Ig (μg/ml) and assayed for TNF-α secretion following incubation with F(ab′)$_2$ GaM. Curves represent the percentage of cytotoxicity as a function of supernatant dilution. (**C** and **D**) Histograms show the binding of IgE^a ICs (C38-2^a) or IgE^b ICs (C48-2^b), (**C**) when diluted 1:2 in normal mouse serum or in PBS to mFcγRIV$^+$ CHO or (**D**) when mFcγRIV$^+$ CHO were preincubated with normal mouse serum diluted 1:2. Solid gray histograms show binding of Ag alone. IC binding was revealed by neutravidin staining. (**E**) mFcγRIV$^+$ CHO were preincubated for 1 hour at 4°C with saturating concentrations of indicated IgG. Curves represent the percentage of IgG2a (open diamonds) or IgG2b (27–35) (filled diamonds) bound to these cells after an incubation at 37°C for increasing time periods. Insets show corresponding histograms at 0 (bold black line), 10 (dark gray line), 30 (black line), and 60 (light gray line) minutes. Solid gray histograms show binding of secondary Abs alone. a-, anti-. (**F**) SPR sensorgrams resulting from the injection of IgG2a or IgG2b (C48-4) onto immobilized mFcγRIV ectodomains. Data are representative of 2 (**A**–**D** and **F**) or 3 (**E**) experiments that gave similar results.

response to IgE^a ICs or to IgE^b ICs (Figure 4E). IgE IC–induced TNF-α secretion was abrogated by preincubating cells with 9G8 or mFcγRIV-blocking mAb 9E9 (Figure 4F and confirmed by anti–TNF-α ELISA in Supplemental Figure 4C).

Human FcεRI(αγ) is a functional equivalent of mouse FcγRIV. In spite of having a high affinity and being expressed on mast cells and basophils, hFcεRI shares with mFcγRIV similar structures and tissue distributions: both can be expressed by monocytes, macrophages, and neutrophils, and they associate with FcRγ, but not FcRβ, in these cells (3). To investigate whether hFcεRI and mFcγRIV could respond similarly to IgE IC, we used hFcεRI^{Tg} mice. As described previously (21), hFcεRI were expressed on the same cells in these mice as in atopic patients. They were detected on blood GR1$^+$ Mac1$^+$ polynuclear cells and GR1$^-$ Mac1$^+$ cells (Figure 5A). They were also detected and with a higher expression on thioglycolate-elicited peritoneal macrophages from transgenic but not from WT mice as described. mFcγRIV was expressed similarly in WT and in hFcεRI^{Tg} macrophages. IgE ICs induced WT macrophages to

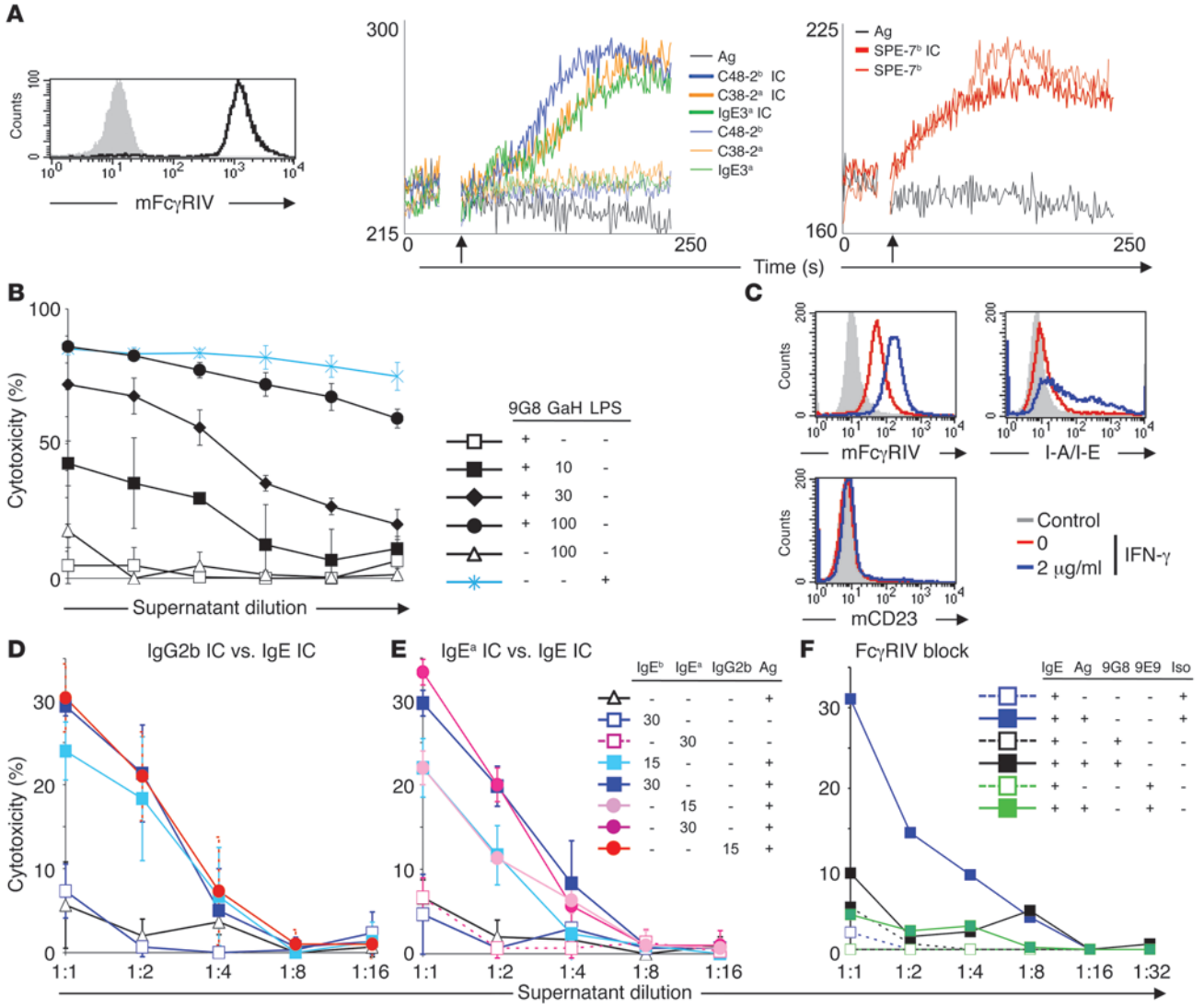

Figure 4

mFcγRIV engagement by IgE ICs induces cell activation in transformed cells. (**A**) The histogram represents the binding of 9G8 to mFcγRIV$^+$ DT40. Transfectants were loaded with Fluo-3, and the intracellular Ca^{2+} concentration was monitored, following triggering (arrows) by Ag alone (black line), IgE alone (thin lines), or IgE ICs (thick lines). Curves represent the relative intracellular Ca^{2+} concentration as a function of time. Two different lots of SPE-7 were assayed and gave similar results. (**B**) TNF-α secreted by MH-S cells, induced by LPS or by 1 μg/ml 9G8 and the indicated concentrations (μg/ml) of goat anti-hamster F(ab′)$_2$ (GaH), was titrated in supernatants. (**C**) Histograms represent the binding of indicated mAbs on IFNγ-treated or untreated MH-S cells. Solid gray histograms represent the binding of isotype controls. (**D** and **E**) TNF-α secreted by IFNγ-treated 2.4G2 F(ab′)$_2$–saturated MH-S cells, induced by the following reagents, was titrated in supernatants: (**D**) IgG2b ICs (Gork) or IgE^b ICs (C48-2^b) and (**E**) IgE^a ICs (C38-2^a) or IgE^b ICs (C48-2^b). (**F**) IFNγ-treated MH-S cells were saturated with both 2.4G2 F(ab′)$_2$ and Polymyxin B–treated 9G8, 9E9, or irrelevant hamster IgG (Iso.). TNF-α secreted by these cells induced by IgE^b ICs (C48-2^b) was titrated in supernatants. Curves represent the percentage of cytotoxicity as a function of MH-S supernatant dilution. All Ig concentrations are indicated in μg/ml. Data are representative of 3 (**A**–**C**) or 2 (**D**–**F**) experiments. Mean ± SD of triplicates in TNF-α bioassays are represented (**B**, **D**, and **E**).

secrete TNF-α. IgE ICs induced hFcεRI^{Tg} macrophages to secrete higher amounts of TNF-α than WT macrophages (Supplemental Figure 5A). To evaluate the contribution of hFcεRI only, we intravenously injected 9E9 into WT or hFcεRI^{Tg} mice and recovered thioglycollate-elicited macrophages. Treatment with 9E9 inhibited 25% of TNF-α secretion by macrophages from hFcεRI^{Tg} mice, while abolishing TNF-α secretion of macrophages from WT mice (Figure 5B and Supplemental Figure 5B). The remaining TNF-α secretion observed in 9E9-treated macrophages from hFcεRI^{Tg} mice corresponds, therefore, to the sole contribution of hFcεRI. Both human FcεRI and murine FcγRIV, therefore, enable macrophages to secrete cytokines in response to IgE ICs.

The engagement of alveolar macrophage mFcγRIV by IgE ICs promotes lung inflammation. FcεRI(αγ) are expressed by human alveolar macrophage in asthmatic patients (22). We therefore examined FcγRIV on mouse alveolar macrophages. CD11c$^+$ Mac-1^{lo} macrophages represent 95% of BAL cells (Figure 6A). BAL cells harvested from *mFcγRIIB*$^{-/-}$*mFcγRIIIA*$^{-/-}$ mice expressed mFcγRIV, but neither

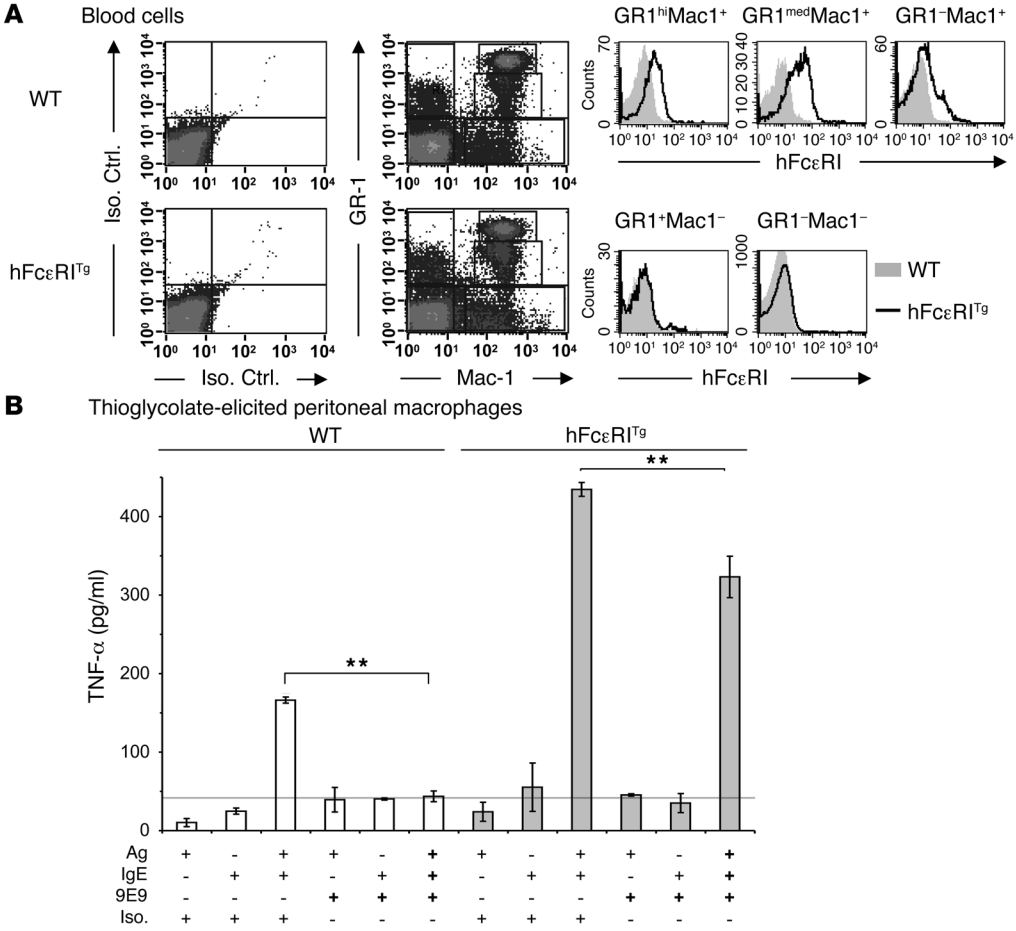

Figure 5

Both hFcεRI and mFcγRIV engagement by IgE ICs induces TNF-α secretion by peritoneal macrophages. (**A**) Density plots show the binding of indicated mAbs to white blood cells from WT and hFcεRI^{Tg} transgenic mice. Histograms show the binding of anti-hFcεRI mAb to cell populations defined by 5 gates from the density plots of blood cells from hFcεRI^{Tg} (open black) or WT (solid gray) mice. (**B**) Indicated mice were injected intravenously with 9E9 or irrelevant hamster IgG 1 day before recovery of thioglycolate-elicited macrophages. The cells were assayed for TNF-α secretion by ELISA following incubation on IgE-, Ag-, or IgE^{b} IC (C48-2^{b})–coated wells. All reagents were treated with Polymyxin B. Mean ± SD of triplicates are represented. Significant differences between cells triggered by IgE^{b} ICs are indicated (**$P < 0.001$; Student's t test). The horizontal gray line represents background TNF-α levels. Data are representative of 3 (**A**) and 2 (**B**) independent experiments.

mFcγRIIB/IIIA, as expected, nor mCD23, and they bound IgE ICs of either allotype. The binding of IgE ICs was abrogated by 9G8 or by 9E9. BAL cells secreted TNF-α when challenged with IgE ICs but not when challenged with monomeric IgE (Figure 6B). WT mouse 2.4G2 F(ab′)$_2$–blocked BAL cells also secreted TNF-α in response to polymyxin-treated IgE ICs, excluding a possible LPS contamination as being responsible for TNF-α secretion (Figure 6C). IgE of the 2 allotypes behaved similarly (Figure 6D).

To determine whether bronchoalveolar macrophage mFcγRIV-dependent IgE-induced signals can induce an inflammatory reaction in vivo, we first used mice lacking mFcεRI and mCD23, the 2 classical IgE receptors. When instilled intranasally (i.n.), IgE ICs induced no significant infiltration of polymorphonuclear cells in the bronchoalveolar space. We hypothesized that mast cell activation is required for initiating the inflammatory response in this model, as it has been described in an autoantibody-dependent arthritis model (23). As the mast cells in the *mFcεRI*$^{-/-}$*mCD23*$^{-/-}$ mice lack the high-affinity receptor for IgE, they cannot be activated by IgE ICs. Therefore, we chose to substitute in vivo airway mast cell activation by i.n. instillation of supernatant of WT BMMCs activated in vitro. Supernatant from high numbers of IgE-sensitized BMMCs challenged with Ag induced a dose-dependent alveolar infiltration, starting at a dose equivalent to 5×10^6 stimulated BMMCs (Figure 7A, 2 left panels). IgE ICs, which failed to induce a significant inflammation when administered alone, induced a robust influx of Mac1$^+$ Gr1$^+$ polynuclear cells in bronchial alveoli when administered to *mFcεRI*$^{-/-}$*mCD23*$^{-/-}$ mice 1 day after an i.n. instillation of a dose of IgE-stimulated BMMC supernatant, which did not induce a detectable inflammation (2.5×10^6 stimulated BMMCs, inducing 1% infiltration, equivalent to the infiltration induced by unstimulated BMMC controls) (Figure 7A, 2 right panels). Because *mFcεRI*$^{-/-}$*mCD23*$^{-/-}$ mice express mFcγRIIB and mFcγRIIIA, which could possibly bind IgE ICs, we repeated the experiments in quintuple-KO mice, which express mFcγRIV only, and as negative controls, in *FcRγ*$^{-/-}$ mice, which express no activating FcR. IgE ICs induced a similar weak infiltration in quintuple-KO and *FcRγ*$^{-/-}$ mice. They induced a marked Mac1$^+$ Gr1$^+$ polynuclear infiltration in quin-

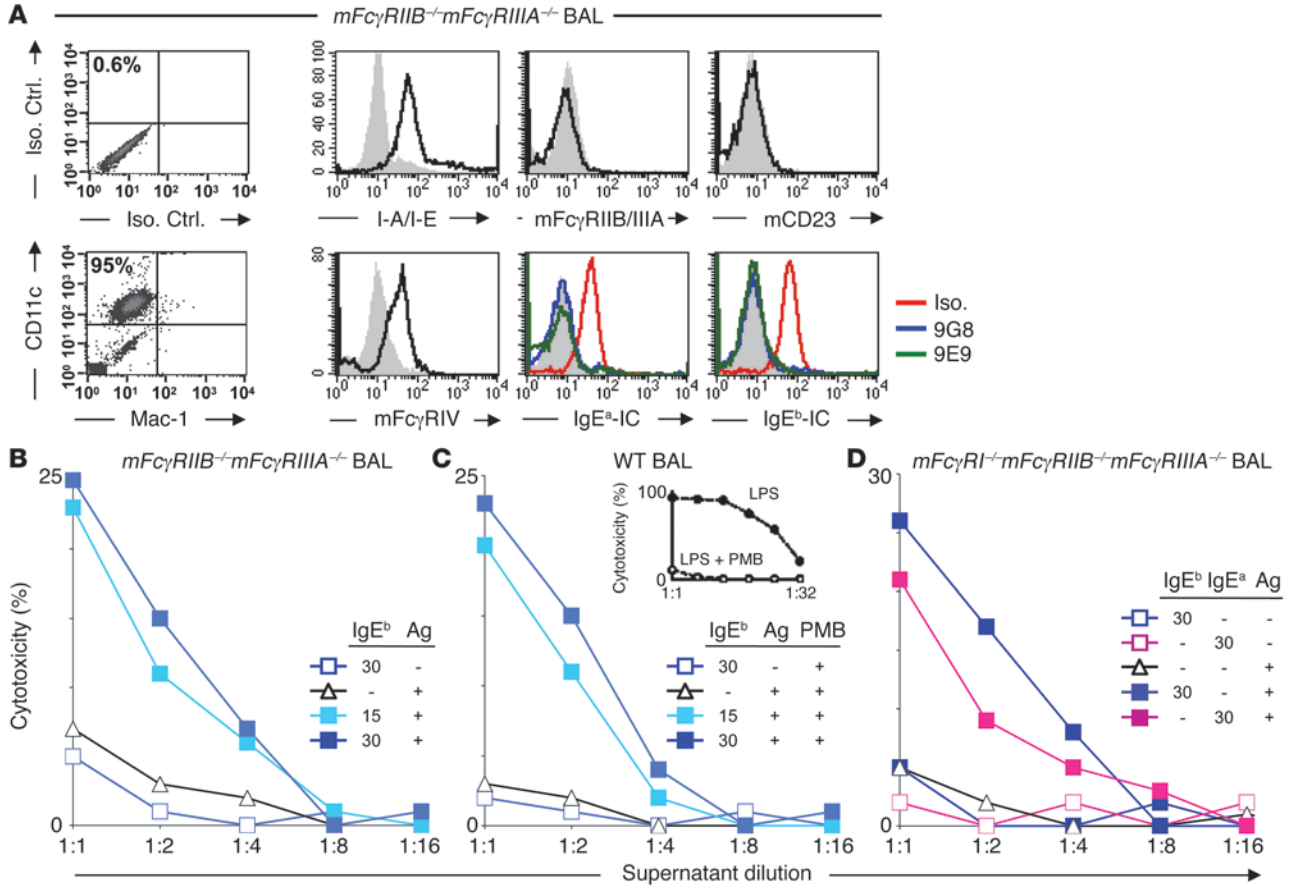

Figure 6

mFcγRIV engagement by IgE ICs induces TNF-α secretion by BAL macrophages. (**A**) Density plots and histograms represent the binding of indicated mAbs, 9E9 anti-mFcγRIV mAb, or isotype controls alone (solid gray histogram, top row) to BAL cells from *mFcγRIIB*$^{-/-}$*mFcγRIIIA*$^{-/-}$ mice, or the binding of IgE^{a} ICs (C38-2^{a}) or IgE^{b} ICs (C48-2^{b}) or Ag alone (TNP_5-BSA-biotin) (solid gray histogram, bottom row). Numbers in the dot plots represent the percentage of cells in the upper-left quadrant. IC binding was revealed by neutravidin staining. IgE IC binding was assayed in the presence or in the absence of 10 μg/ml 9G8, 9E9, or irrelevant hamster IgG. (**B**–**D**) TNF-α secreted by BAL macrophages, harvested from indicated mice and induced by the following reagents, was titrated in supernatants: (**B**) IgE^{b} ICs (C48-2^{b}) or (**C**) Polymyxin B–treated (PMB-treated) IgE^{b} ICs (C48-2^{b}) or (**D**) IgE^{a} ICs (C38-2^{a}) or IgE^{b} ICs (C48-2^{b}). The effect of (open circles) Polymyxin B treatment on (filled circles) 1 ng/ml LPS-induced TNF-α secretion is shown in inset. Curves represent the percentage of cytotoxicity as a function of supernatant dilution. Ig concentrations are indicated in μg/ml. Data are representative of 2 (**A**, **B**, and **D**) independent experiments that gave similar results.

tuple-KO (Figure 7B) but not in *FcRγ*$^{-/-}$ mice (Figure 7C) when administered after a dose of IgE-stimulated BMMC supernatant, which induced no detectable infiltration. No significant increase in lymphocyte populations in the BALs from quintuple-KO mice could be observed, either by flow cytometry (BMMC supernatant, 0.10% ± 0.03%; IgE-ICs, 0.09% ± 0.06%; BMMC supernatant plus IgE-ICs, 0.17% ± 0.10%; variations not significant, Student's *t* test) or by cytospin analysis (data not shown). Mediators released by IgE-sensitized mast cells upon engagement of FcεRI by Ag can, therefore, enable bronchoalveolar macrophages to induce lung infiltration, upon engagement of FcγRIV by IgE ICs.

Discussion

mFcγRIV shares several properties with hFcγRIIIA (hCD16A) and, for this reason, it was first named CD16-2 (1). mFcγRIV was found to have an intermediate affinity for mouse IgG2a ($K_A = 2.9 \times 10^7\ M^{-1}$) and IgG2b ($K_A = 1.7 \times 10^7\ M^{-1}$) (2). hFcγRIIIA was also found to have an intermediate affinity for human IgG ($K_A \approx 2.5 \times 10^7\ M^{-1}$) (24, 25). The higher affinity of hFcγRIIIA than that of hFcγRIIIB was proposed to result from the association of hFcγRIIIA with the FcRγ subunit (26). This association confers on mFcγRIV and hFcγRIIIA their cell-activating properties. The high amino acid sequence homology (64.9%) of the extracellular domains of mFcγRIV and hFcγRIIIA may also account for their similar intermediate affinities for IgG. These common features, altogether, support the current view that hFcγRIIIA is a human equivalent of murine FcγRIV. Our data challenge this view.

We show here that mFcγRIV is an IgE receptor. IgE ICs, but not monomeric IgE, bound to mFcγRIV. This was observed on mFcγRIV^{+} CHO, transformed macrophagic cells, BM-derived cultured macrophages (data not shown), and freshly isolated ex vivo BAL macrophages. IgE^{a} and IgE^{b} bound to all 4 cell types similarly. When measured by SPR analysis, the mean affinity of mFcγRIV for 5 different IgE was $K_A \approx 4 \times 10^5\ M^{-1}$. IgE^{a} and IgE^{b} bound with the same affinities. These data, altogether, identify mFcγRIV as a low-affinity receptor for IgE, irrespective of IgE allotypes. Inter-

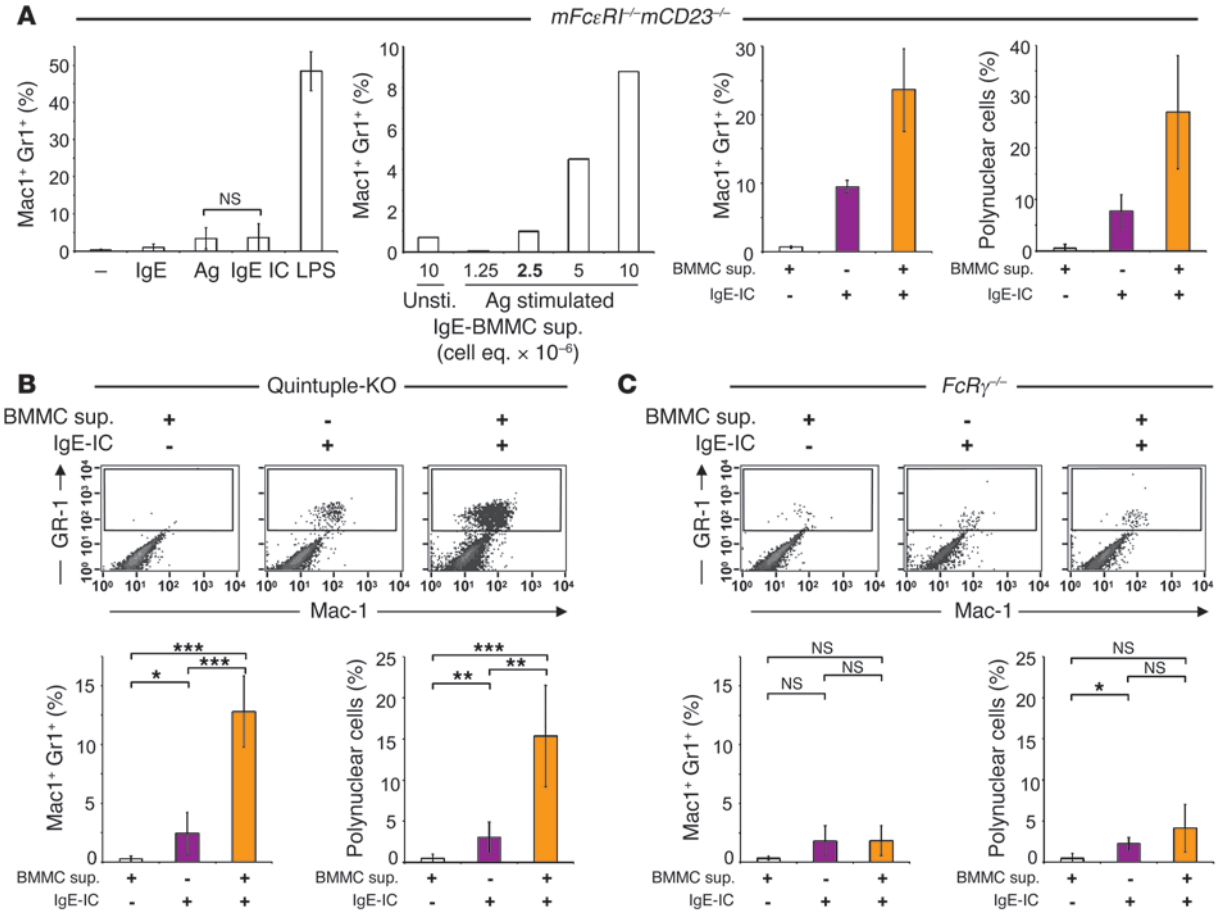

Figure 7

mFcγRIV engagement by IgE ICs in vivo promotes lung infiltration. (**A**) *mFcεRI*$^{-/-}$*mCD23*$^{-/-}$ mice were instilled i.n. with IgE^{a} anti-OVA (2C6^{a}), Ag (OVA), preformed IgE^{a} ICs (2C6^{a}-OVA) ($n = 7$), or LPS ($n = 2$) (first panel), or with cell-free supernatants corresponding to indicated numbers of unstimulated (Unsti.) or activated WT BMMCs (cell equivalent [eq.] × 10^{-6}) ($n = 2$) (second panel) on day 0. Bold is used to indicate the dose used in **B** and **C**. *mFcεRI*$^{-/-}$*mCD23*$^{-/-}$ mice were instilled i.n. with the same cell-free supernatants (sup.) corresponding to 2.5 × 10^6 activated BMMCs on day 0 (a dose that does not induce a significant infiltration [1%] compared with that induced by supernatant from unstimulated BMMCs) and with preformed IgE^{a} ICs on day 1 as indicated. Bar graphs represent the percentage of Mac1^{+} Gr1^{+} in BAL from these mice 24 hours after i.n. instillation (3 left panels) or the percentage of polynuclear cells in cytospins of BAL (right panel) on day 3. (**B** and **C**) Quintuple-KO ($n = 5$) or *FcRγ*$^{-/-}$ ($n = 3$) mice were instilled i.n. with the same cell-free supernatants as in **A**, corresponding to 2.5 × 10^6 activated BMMCs on day 0, and with preformed IgE^{a} ICs (2C6^{a}-OVA) on day 1. A representative density plot of BAL cells from these mice on day 2 for each experimental condition is shown. Bar graphs represent the percentage of Mac1^{+} Gr1^{+} in BAL or the percentage of polynuclear cells in cytospins of BAL. Error bars represent mean ± SD (**A**–**C**) and significant differences between sample means are indicated (***$P < 0.001$; **$P \leq 0.01$; *$P < 0.05$; n.s., $P > 0.05$; Student's t test).

estingly, 2 amino acids (K_{117} and E_{132}) (27), which are involved in the formation of 2 salt bridges between the extracellular domains of hFcεRI and the Fc portion of human IgE and which are critical for the binding of IgE, are conserved in mFcγRIV. mFcγRIV was recently reported to bind mouse IgE^{b} but not IgE^{a} (10). We found the same preference for IgE^{b} when using the same commercially available IgE under the same conditions, i.e., when not ultracentrifuged and at the same high concentrations. Binding of IgE of both allotypes, however, was abrogated when aggregates were removed by ultracentrifugation. The 2 IgE^{b} anti-DNP, SPE-7 and C48-2, were reported to spontaneously aggregate and to activate mast cells in the absence of Ag (28). Aggregates present in higher amounts in IgE^{b} preparations could account for the preference of mFcγRIV for nonultracentrifuged IgE^{b} observed by Hirano et al. (10) and by us. In contrast with mFcγRIV, hFcγRIIIA is not an IgE receptor. hFcγRIIIA had no measurable affinity for human IgE when studied by SPR, and human IgE failed to bind to hFcγRIII^{+} CHO, whether as monomers or as F(ab′)$_2$–anti-human F(ab′)$_2$ complexes. hFcγRIIIA and hFcγRIIIB gave similar results, irrespective of known polymorphisms.

We also found that IgG2a and IgG2b monomers bind to mFcγRIV and that mFcγRIV-bound IgG2 triggers cytokine secretion when crosslinked on ex vivo macrophages. mFcγRIV therefore fulfills the criteria defining high-affinity receptors. If so, one expects mFcγRIV to be occupied by IgG in vivo. mFcγRIV may therefore not be available for IgE ICs, especially as the concentration of IgG is much higher than that of IgE in vivo. However, we found that IgG2a/2b rapidly dissociated from mFcγRIV at 37°C and that IgE ICs replaced IgG2a when added to IgG-saturated mFcγRIV^{+} CHO. This finding is of critical importance as it provides a possible biological significance to mFcγRIV as a low-affinity receptor for IgE.

The ITAM-containing FcRγ subunit provides mFcγRIV with cell-activating properties. IgE ICs triggered an increase in the intracellular Ca^{2+} concentration in mFcγRIV$^+$ DT40 cells. IgE^a and IgE^b induced similar Ca^{2+} responses. As expected, the anti-DNP IgE^b SPE-7 also triggered Ca^{2+} responses in the absence of Ag, supporting the interpretation that it spontaneously aggregates. Noticeably, SPE-7 contained qualitatively bigger aggregates than other IgEs tested by dynamic light scattering. We also observed that, differing from all other IgE tested, SPE-7 bound to mFcγRI. SPE-7 has been reported previously to exhibit Ag multiplicity, binding other molecules than DNP and IgE-binding molecules, to preexist in 2 different conformations, and to exist as 4 different conformations in the presence of Ag (29). It has also been reported that SPE-7 activates mast cells in the absence of Ag (28, 30), but that monovalent hapten abolishes these properties (31), suggesting that SPE-7 auto-aggregates due to a low affinity for its own structure and/or recognizes other cell surface components (32) (reviewed in ref. 33). Altogether, these data obtained by others strongly support our data that SPE-7 contains high–molecular weight aggregates, induces activation in the absence of Ag, and binds other molecules than DNP and IgE-binding molecules, including mFcγRI. Data obtained with this mAb could be questionable, especially when used at high local concentrations in vitro and in vivo: a local injection may considerably affect the probability of high local concentrations of SPE-7 aggregates compared with a systemic (intravenous) injection and therefore induce or not induce cross binding to other molecules.

In addition to triggering calcium responses, IgE ICs triggered TNF-α secretion by a macrophage cell line, MH-S, and by ex vivo macrophages. IgE^a and IgE^b ICs induced the secretion of similar amounts of TNF-α. The TNF-α secretion was due to mFcγRIV, as responses of both cell types were not affected by 2.4G2 F(ab′)$_2$, while responses of MH-S were abolished by 9G8. ICs made of IgG2 ICs and IgE ICs induced TNF-α secretions of similar intensities, indicating that they bound to mFcγRIV with similar avidities, although mFcγRIV has markedly different affinities for IgG2 and IgE. IgE ICs can therefore activate macrophages via mFcγRIV. IgE ICs may form when IgE is synthesized locally. A local IgE production was described in the upper respiratory tract of atopic patients and in the bronchial mucosa of asthmatic patients (34). Antibody class-switching to IgE, and therefore local IgE production, is enhanced locally in the nasal mucosa in grass pollen-allergic subjects suffering from rhinitis during the pollinic season (35). They can also form in helminth infections, in which specific IgE and parasite Ag are present in high concentrations.

Human macrophages do not express FcγRIV. They can, however, express another IgE receptor, hFcεRI. Although hFcεRI has a high affinity whereas mFcγRIV has a low affinity for IgE, both can be engaged by IgE ICs. Moreover, hFcεRI is expressed without FcRβ in macrophages and neutrophils and especially in atopic patients (13, 22). Mouse macrophage/neutrophil FcγRIV and human macrophage/neutrophil FcεRI(αγ) therefore have the same quaternary structure: an IgE-binding subunit and the same ITAM-containing FcRγ subunit. hFcεRI expressed in macrophages from transgenic mice triggered TNF-α to a similar extent as mFcγRIV when engaged by IgE ICs. mFcγRIV and hFcεRI have therefore similar functional properties. hFcεRI aggregation was described to trigger Ca^{2+} responses and cytokine secretion in monocytes from atopic patients (13) and in neutrophils from asthmatic patients (14). As hFcεRI(αγ) is overexpressed on monocytes, neutrophils, and eosinophils in atopic patients and particularly on alveolar macrophages (22), we examined freshly isolated BAL cells for mFcγRIV expression and function. BAL macrophages from WT, *mFcγRIIB/IIIA*$^{-/-}$, and *mFcγRI/IIB/IIIA*$^{-/-}$ mice expressed mFcγRIV, but neither mFcεRII (mCD23) nor mFcεRI. Binding of IgE ICs to these cells was mFcγRIV dependent, as binding was abolished by 9G8 or 9E9. IgE ICs, but not monomeric IgE, induced these BAL cells to secrete TNF-α. Comparable results were obtained with BAL cells from *mFcγRI/IIB/IIIA*$^{-/-}$ mice. IgE^a ICs and IgE^b ICs gave similar results. These IgE-induced, mFcγRIV-dependent biological responses of alveolar macrophages are of potentially high physiological relevance. TNF-α, which induces bronchial hyperresponsiveness (36), airway infiltration by neutrophils and eosinophils (37), and activates airway smooth muscle (38), was indeed recognized as playing a major role in asthma-associated remodeling and pulmonary inflammation, especially in asthma refractory to corticosteroid therapy (39).

These results prompted us to examine the role of mFcγRIV in a murine model of passive lung inflammation. Surprisingly, while IgE ICs did induce a weak influx of polynuclear cells in BAL (8%–10%) when instilled i.n. in *mFcεRI*$^{-/-}$*mCD23*$^{-/-}$ mice, they did induce an almost undetectable influx (2.5%) when instilled i.n. in quintuple-KO mice. Therefore, IgE-ICs may induce some infiltration in BAL by triggering mFcγRIIIA on mast cells. Lung inflammation involves multiple cell types. Among these, mast cells are well known as the initiators of IgE-induced allergic reactions. We therefore "primed" mice by instilling i.n. supernatants of IgE-sensitized mast cells challenged with Ag in vitro. Mast cell supernatants, collected 30 minutes after challenge, contained granular and lipid mediators but low levels of cytokines (e.g., 92 ± 6 pg/ml TNF-α). These supernatants induced a dose-dependent lung infiltration of polynuclear cells in *mFcεRI*$^{-/-}$*mCD23*$^{-/-}$ mice. Supernatants from high numbers of activated mast cells were required for inducing a significant infiltration. When administered i.n. at a dose which induced no detectable inflammation, supernatants from activated mast cells enabled IgE ICs to induce a marked lung infiltration not only in mFcεRI- and mCD23-deficient mice, but also in quintuple-KO mice, which express mFcγRIV only, but not in FcRγ-deficient mice, which express no activating FcR. The absence of inflammation observed in FcRγ-deficient mice rules out the participation of IgE-binding molecules that are not associated with the FcRγ chain, e.g., galectin-3 (40). The use of quintuple-KO mice excluded the contributions not only of the 2 main IgE receptors (mFcεRI and mCD23) but also those of the 2 "minor" IgE receptors (mFcγRIIB and mFcγRIIIA) to the inflammatory process we observed. It leaves mFcγRIV as the sole candidate among all known FcRs. mFcγRIV-expressing cells may therefore synergize with mFcεRI-expressing mast cells to generate an IgE-induced lung inflammation. Whether unidentified products in mast cell supernatant enhanced the responsiveness of mFcγRIV-expressing macrophages to IgE ICs, whether vasoactive mediators initiated the extravasation of polynuclear cells into tissues, or whether secreted proteases facilitated their migration by degrading the extracellular matrix is unknown. The responsible mediators in supernatants from activated BMMCs may not be mast cell specific; other cells could, however, possibly cooperate with macrophages in vivo.

In conclusion, we demonstrate here that mFcγRIV is a low-affinity receptor for IgE, irrespective of allotypes. It can therefore operate in all mouse strains. mFcγRIV has the same quaternary structure, the same tissue distribution, the same ligands, and the same functional properties as human FcεRI(αγ). Mice may therefore

be a better model for IgE-dependent inflammation, allergies, and parasite infections than previously thought, macrophage FcγRIV playing, in murine models, the role played by macrophage FcεRI in patients. The cooperation between mast cells and mFcγRIV-expressing lung cells proposed here in a mouse model of IgE-induced lung inflammation, indeed suggests that a similar cooperation may occur between mast cells and hFcεRI-expressing lung cells in allergic asthma.

Methods

Cells and cDNAs. CHO-K1, HEK293T, DT40, and MH-S cells were from the ATCC and cultured as recommended by the manufacturer. BMMCs were obtained from mouse BM cells cultured in OptiMEM (Invitrogen) in 10% FCS, supplemented with 5% X63-IL3–conditioned medium for 4 weeks (≥ 90% mast cells).

cDNAs coding for mouse FcγRI, FcγRIIB1 (Ly17.2 haplotype), FcγRIIIA (H haplotype; ref. 41), and FcRγ were previously cloned in the laboratory. cDNA from C57BL/6 and 129/Sv spleen cells were used to clone mFcγRIV and mFcγRIIB1 (Ly17.1), respectively. Both mFcγRIIB1 haplotypes gave identical results throughout this study; only results obtained with Ly17.2 haplotype are presented. Human FcγRI and FcγRIIA(R_{131}) cDNAs were from J. Van de Winkel and J. Leusen (University Medical Center Utrecht, Utrecht, The Netherlands). hFcγRIIIB (NA1, NA2, or SH) cDNAs were provided by S. Santoso and U. Sachs (Institute for Clinical Immunology and Transfusion Medicine, Giessen, Germany). cDNA from human blood cells were used to clone hFcγRIIIA(V_{176}), and hFcγRIIIA(F_{176}) by site directed mutagenesis. A cDNA sequence coding for a FLAG tag was inserted immediately 3′ of the signal sequence cleavage site in all FcR cDNAs. Resulting constructs were cloned into pNT (neomycin^R). cDNAs corresponding to EC domains of all FcRs were cloned into p3xFLAG-CMV-14 (Sigma-Aldrich). Stable transfectants were obtained and sorted to equivalent surface expression by flow cytometry on a MoFlo (Dako) or FACSAria (Becton Dickinson).

Mice. *mFcγRIIB/IIIA*$^{-/-}$ and *mFcγRI/IIB/IIIA*$^{-/-}$ C57BL/6 (N5 B6) mice (42) were provided by S. Verbeek (Leiden University Medical Center, Leiden, The Netherlands) and backcrossed to generation N8. hFcεRI^{Tg} (N6 B6) and mFcεRI-deficient (43) (N5 B6) mice were provided by J.-P. Kinet (Harvard Institutes of Medicine, Boston, Massachusetts, USA) and backcrossed to N12 B6. mCD23-deficient (44) (N12 B6) mice were provided by M. Lamers (Max-Planck-Institute for Immunobiology, Freiburg, Germany). Quintuple-KO (N6 B6) mice were obtained by intercrosses. WT C57BL/6J and 129/Sv were purchased from Charles River Laboratories, and *FcRγ*$^{-/-}$ mice (N12 B6) were purchased from The Jackson Laboratories. BALs were performed on ketamin-xyalizin anesthetized mice, using 6 washes of 1 ml normal saline solution, and cells were purified by adherence. Peritoneal macrophages were harvested from mice injected i.p. with 2 ml thioglycollate (Bio-Rad) 4–5 days prior to harvest and purified by adherence. All mouse protocols were approved by the Animal Care and Use Committees of Comité régional d'éthique en matière d'expérimentation animale, Ile-de-France, France.

mAbs and reagents. Mouse IgEs, anti–2,4,6-trinitrophenyl hapten (anti-TNP) mIgEs (C38-2^a, C48-2^b, 15.3.2^a) and anti-dansyl mIgE^a (27-74^a), were purchased from BD Biosciences — Pharmingen; anti-DNP mIgE^b (SPE-7^b) was purchased from Sigma-Aldrich; mouse IgE^a anti-OVA (2C6^a) were provided by L. Kobzik (Harvard School of Public Health, Boston, Massachusetts, USA) (45); and the mouse IgE^a anti-DNP mAb 2682-I^a was used as culture supernatant. All these IgEs were purified from culture supernatants of hybridomas by the manufacturers or in house and cannot therefore contain another allotype of IgE. Several batches of each commercial IgE were used and gave identical results.

FITC-conjugated mIgG1 and FITC-conjugated mIgG2a, anti-dansyl mIgG2b (27-35), anti-KLH mIgG2b (C48-4), anti-mFcγRIIB/IIIA (2.4G2), FITC-conjugated rat anti-mIgG2a, FITC-conjugated anti-Mac1, FITC-conjugated anti-hFcεRI, PE-conjugated anti-I^A/I^E, PE-conjugated anti-mCD23, PE-conjugated anti-Gr1, and hamster IgG were purchased from PharMingen; unlabeled-, HRP- or FITC-labeled anti-FLAG (M2) and LPS were purchased from Sigma-Aldrich; unlabeled and FITC-labeled F(ab′)$_2$ GaM were purchased from Jackson ImmunoResearch Laboratories Inc.; PE-conjugated neutravidin was purchased from Molecular Probes; and unlabeled and FITC-labeled F(ab′)$_2$ goat anti-hamster (GaH) were purchased from Serotec. Hamster anti-mFcγRIV mAb 9G8 and 9E9 were provided by J.V. Ravetch (The Rockefeller University, New York, New York, USA); mIgG1 anti-TNP (D10), mIgG2b anti-TNP (GORK), and mIgG2a anti-SRBC (12-6-22) mAbs were provided by B. Heyman (Uppsala Universitet, Uppsala, Sweden); and human myeloma IgE PS was provided by T.F. Huff (Virginia Commonwealth University, Richmond, VA, USA). Recombinant murine IFN-γ was purchased from Peprotech, and low-endotoxin lysozyme-free OVA was purchased from MP Biomedicals. BSA was trinitrophenylated using trinitrobenzene sulfonic acid to 5 or 16 moles of TNP per mole of BSA.

Monomeric Ig binding assays. Aggregates in stock solutions were removed by an 18-hour ultracentrifugation at 100,000 *g*, and 2×10^5 cells were incubated with monomeric Ig at indicated concentrations for 1 hour at 4°C. Cell-bound Ig was detected using 15 μg/ml F(ab′)$_2$ FITC-conjugated GaM or PE-conjugated F(ab′)$_2$ anti-human F(ab′)$_2$-specific Abs for 30 minutes at 4°C.

IC Ig binding assays. Unless otherwise specified, mouse ICs were preformed by incubating 10 μg/ml TNP_{16}-BSA-biotin with 30 μg/ml anti-TNP mAbs for 1 hour at 37°C, and 2×10^5 cells were incubated with ICs for 2 hours at 4°C. ICs bound to cells were detected using PE-conjugated neutravidin at 2 μg/ml for 30 minutes at 4°C.

Serum or monomeric IgG2a versus IgE IC competition assay. A total of 2×10^5 cells were incubated successively with serum diluted 1:2 or with 30 μg/ml mIgG2a (12-6-22), washed, and incubated with IgE ICs for 2 hours at 4°C; or incubated simultaneously with IgE ICs diluted 1:2 in normal mouse serum; or incubated with both mIgG2a and IgE ICs for 2 hours at 4°C. Bound mIgG2a was revealed using 5 μg/ml FITC-conjugated F(ab′)$_2$ anti-mIgG2a, and bound IgE ICs were revealed using PE-conjugated neutravidin for 30 minutes at 4°C. Saturation of mFcγRIV by mIgG2a or mIgG2b was obtained from the concentration of 30 μg/ml and up (data not shown).

Dynamic light scattering. Untreated or ultracentrifuged IgE solutions at 300 μg/ml in PBS were analyzed immediately after ultracentrifugation for homogeneity and presence of aggregates of high molecular weight, using a DynaPro MS800 dynamic light scattering instrument (Wyatt). Triplicates of 20 measurements at 25°C were averaged with acquisition periods of 10 seconds. During the illumination, the photons scattered by proteins were collected at a 90-degree angle on a 10-second acquisition period and were fit with the analysis software Dynamics (Wyatt). Intensity fluctuations of the scattered light, resulting from Brownian motion of particles, were analyzed with an autocorrelator to fit an exponential decay function, then measuring a translational diffusion coefficient D. For polydisperse particles, the autocorrelation function was fit as the sum of contributions from the various size particles using the regularization analysis algorithm. *D* is converted to a hydrodynamics radius *Rh* through the Stokes-Einstein equation ($Rh = k_bT/6\pi\eta D$, where η is the solvent viscosity, k_b is the Boltzmann's constant, and *T* is the temperature). Apparent molecular weights for a spherical particle were deduced from histograms of distribution of percent intensity versus radius to identify the peak containing monomeric IgE.

Measurement of intracellular free calcium concentration. Mobilization of intracellular free calcium concentration was determined as described previously (46).

Secretion of TNF-α in MH-S and BAL macrophages. For 4 hours, 2.4×10^5 MH-S cells or 1.2×10^5 alveolar macrophages were incubated with indicated

reagents at 37°C. If indicated, preincubations were performed for 1 hour at 4°C: mFcγRIIB/mFcγRIIIA were blocked by 20 μg/ml 2.4G2 F(ab′)$_2$ or mFcγRIV was blocked by 10 μg/ml 9G8 or 9E9. If indicated, reagents were preincubated 1 hour at 37°C in the presence of 2 μg/ml Polymyxin B.

Secretion of TNF-α in peritoneal macrophages. All plates were coated in sodium carbonate, with or without the presence of 100 μg/ml TNP_{16}-BSA containing 2 μg/ml Polymyxin B, saturated with 1 mg/ml BSA, and incubated with 30 μg/ml IgE^b anti-TNP (C48-2^b) or without for 1 hour at 37°C. Cells were preincubated in the presence of 20 μg/ml 2.4G2 F(ab′)$_2$, added to wells, and incubated for 3 hours at 37°C. For peritoneal macrophages from quintuple-KO mice, cells were incubated for 1 hour with monomeric Ig as indicated, washed 3 times, and incubated with 15 μg/ml F(ab′)$_2$ GaM for 3 hours at 37°C. If indicated, mice were injected intravenously with 20 μg Hamster anti-mFcγRIV mAb 9E9 or irrelevant Hamster IgG 1 day before macrophage harvest.

Serial dilutions of cell-free supernatants were harvested and titrated for TNF-α by a cytotoxic assay on L929 cells that could be abrogated by anti–TNF-α mAbs as described previously (47). Additionally, TNF-α was titrated using an anti–TNF-α ELISA kit (R&D Systems).

Production of soluble FcR ectodomains tagged with 3xFLAG fusion protein. cDNA constructs coding for soluble FcR ectodomains tagged with a 3xFLAG peptide were transfected by a standard calcium chloride technique into HEK293T cells. Fusion proteins from 96-hour supernatants were purified on anti-FLAG agarose beads and eluted using 3xFLAG peptide. Purity of PNGase F–treated or untreated proteins was assessed after SDS-PAGE by anti-FLAG M2-HRP blotting and revealed using ECL reagents.

SPR analysis. A BIAcore 2000 SPR biosensor (Biacore) was used to assay the interaction of soluble ectodomains of FcR with monoclonal Ig. An *N*-hydroxysuccinimide ester was formed on a CM5 sensorchip surface. Ectodomains were immobilized at acidic pH. mFcγRI, mFcγRIIB, mFcγRIIIA, and mFcγRIV ectodomains were immobilized to 1,700; 3,365; 3,161; and 2,890 RU respectively, and hFcεRI ectodomains were immobilized to 780 RU. Regeneration was performed using 10 mM NaOH. Aggregates in stock solutions of commercial IgE were separated from monomeric Ig using Ultrafree-CL PTMK Ultracel-PL 300-kDa Cut-off spin columns (Millipore). (As an internal control of the experiment, 100% of mouse IgM anti-TNP was retained on the column.) A range of Ig concentrations was injected into flow cells at a flow rate of 20 μl/min, with a contact and dissociation time of 150 seconds and 300–500 seconds, respectively. Binding response was recorded as RU (1 RU ≈ 1 pg/mm^2) continuously, background binding was automatically subtracted, and equilibrium dissociation constant (K_D) values were calculated either from the steady state values reached at the end of the injection or from association rate constant and dissociation rate constant values when determined using BIAevaluation v4.2 software (Biacore). A 1:1 Langmuir binding model closely fitted the observed sensorgram data and was used in all experiments.

In vivo lung inflammation model. BMMCs, sensitized overnight at 37°C with 0.1 μg/ml IgE^a anti-DNP (clone 2682 I^a) or not, were washed, and challenged for 30 minutes at 37°C with 10 ng/ml DNP_{15}-BSA. Ketamin-xyalizin anesthetized mice were instilled i.n. with 30 μl supernatant, corresponding to indicated numbers of BMMCs or with 30 μl saline on day 0. On day 1, IgE^a ICs, preformed 1 hour at 37°C and made of 30 μg/ml IgE^a anti-OVA (clone 2C6^a) and 1 μg/ml OVA or saline were instilled i.n. On day 2, BAL were performed and analyzed by flow cytometry, following staining with anti-Mac1/anti-Gr1 mAbs, and by microscopy, following Diff-Quick staining of cytospins.

Statistics. Statistical analysis was performed using 1-tailed Student's *t* test. Results are expressed as the mean ± SD. *P* values of less than 0.05 were considered significant.

Acknowledgments

We are thankful to our colleagues for their generous gifts: S. Verbeek, J.-P. Kinet, and M. Lamers for mice; B. Heyman, J.V. Ravetch, L. Kobzik, and T.F. Huff for mAbs; and J. Van de Winkel, J. Leusen, S. Santoso, and U. Sachs for cDNAs. We thank A. Louise and H. Kieffer-Biasizzo (Plate-Forme de Cytométrie, Institut Pasteur, Paris) for cell sorting and R. Kapetanovic (Unité de recherche Cytokines et Inflammation, Institut Pasteur, Paris) for training in BAL techniques. D.A. Mancardi is the recipient of a fellowship from the Ministère de l'Enseignement Supérieur et de la Recherche. This work was supported by the Institut Pasteur and INSERM and by grants from Agence Nationale de la Recherche (ANR) (05-JCJC-0236-01), Fondation pour la Recherche Médicale (FRM) (Défis de la Recherche en Allergologie), and the MUGEN European Network of Excellence.

Received for publication June 11, 2008, and accepted in revised form September 10, 2008.

Address correspondence to: Pierre Bruhns, Unité d'Allergologie Moléculaire et Cellulaire, Département d'Immunologie, Institut Pasteur, 25 rue du Docteur Roux, 75015 Paris, France. Phone: 33-1-4568-8629; Fax: 33-1-4061-3160; E-mail: bruhns@pasteur.fr.

1. Mechetina, L.V., Najakshin, A.M., Alabyev, B.Y., Chikaev, N.A., and Taranin, A.V. 2002. Identification of CD16-2, a novel mouse receptor homologous to CD16/Fc gamma RIII. *Immunogenetics.* **54**:463–468.
2. Nimmerjahn, F., Bruhns, P., Horiuchi, K., and Ravetch, J.V. 2005. Fc gamma RIV: a novel FcR with distinct IgG subclass specificity. *Immunity.* **23**:41–51.
3. Daëron, M. 1997. Fc receptor biology. *Annu. Rev. Immunol.* **15**:203–234.
4. Lin, S., Cicala, C., Scharenberg, A.M., and Kinet, J.P. 1996. The Fc epsilon RI beta subunit functions as an amplifier of Fc epsilon RI gamma-mediated cell activation signals. *Cell.* **85**:985–995.
5. Ra, C., Jouvin, M.H., Blank, U., and Kinet, J.P. 1989. A macrophage Fc gamma receptor and the mast cell receptor for IgE share an identical subunit. *Nature.* **341**:752–754.
6. Kinet, J.P., et al. 1988. Isolation and characterization of cDNAs coding for the beta subunit of the high-affinity receptor for immunoglobulin E. *Proc. Natl. Acad. Sci. U. S. A.* **85**:6483–6487.
7. Kurosaki, T., Gander, I., Wirthmueller, U., and Ravetch, J.V. 1992. The beta subunit of the Fc epsilon RI is associated with the Fc gamma RIII on mast cells. *J. Exp. Med.* **175**:447–451.
8. Blank, U., et al. 1989. Complete structure and expression in transfected cells of high affinity IgE receptor. *Nature.* **337**:187–189.
9. Miller, L., Blank, U., Metzger, H., and Kinet, J.P. 1989. Expression of high-affinity binding of human immunoglobulin E by transfected cells. *Science.* **244**:334–337.
10. Hirano, M., et al. 2007. IgE(b) immune complexes activate macrophages through Fc gamma RIV binding. *Nat. Immunol.* **8**:762–771.
11. Borges, M.S., Kumagai, Y., Okumura, K., and Tada, T. 1981. Genetic polymorphism (Igh-7 allotype) detected on murine IgE. *Int. Arch. Allergy Appl. Immunol.* **66**(Suppl. 1):51–54.
12. Shinkai, Y., Nakauchi, H., Honjo, T., and Okumura, K. 1988. Mouse immunoglobulin allotypes: multiple differences between the nucleic acid sequences of the IgEa and IgEb alleles. *Immunogenetics.* **27**:288–292.
13. Maurer, D., et al. 1994. Expression of functional high affinity immunoglobulin E receptors (Fc epsilon RI) on monocytes of atopic individuals. *J. Exp. Med.* **179**:745–750.
14. Gounni, A.S., et al. 2001. Human neutrophils express the high-affinity receptor for immunoglobulin E (Fc epsilon RI): role in asthma. *FASEB J.* **15**:940–949.
15. Takizawa, F., Adamczewski, M., and Kinet, J.P. 1992. Identification of the low affinity receptor for immunoglobulin E on mouse mast cells and macrophages as Fc gamma RII and Fc gamma RIII. *J. Exp. Med.* **176**:469–475.
16. Ravetch, J.V., and Perussia, B. 1989. Alternative membrane forms of Fc gamma RIII (CD16) on human natural killer cells and neutrophils. Cell type-specific expression of two genes that differ in single nucleotide substitutions. *J. Exp. Med.* **170**:481–497.
17. Ory, P.A., et al. 1989. Sequences of complementary DNAs that encode the NA1 and NA2 forms of Fc receptor III on human neutrophils. *J. Clin. Invest.* **84**:1688–1691.

18. Bux, J., et al. 1997. Characterization of a new alloantigen (SH) on the human neutrophil Fc gamma receptor IIIb. *Blood.* **89**:1027–1034.
19. Dombrowicz, D., et al. 1996. Anaphylaxis mediated through a humanized high affinity IgE receptor. *J. Immunol.* **157**:1645–1651.
20. Warmerdam, P.A., van de Winkel, J.G., Gosselin, E.J., and Capel, P.J. 1990. Molecular basis for a polymorphism of human Fc gamma receptor II (CD32). *J. Exp. Med.* **172**:19–25.
21. Dombrowicz, D., et al. 1998. Allergy-associated FcR beta is a molecular amplifier of IgE- and IgG-mediated in vivo responses. *Immunity.* **8**:517–529.
22. Ochiai, K., et al. 1996. Expression of high-affinity IgE receptor (Fc epsilon RI) on human alveolar macrophages from atopic and non-atopic patients. *Int. Arch. Allergy Immunol.* **111**(Suppl. 1):55–58.
23. Lee, D.M., et al. 2002. Mast cells: a cellular link between autoantibodies and inflammatory arthritis. *Science.* **297**:1689–1692.
24. Vance, B.A., Huizinga, T.W., Wardwell, K., and Guyre, P.M. 1993. Binding of monomeric human IgG defines an expression polymorphism of Fc gamma RIII on large granular lymphocyte/natural killer cells. *J. Immunol.* **151**:6429–6439.
25. Edberg, J.C., and Kimberly, R.P. 1997. Cell type-specific glycoforms of Fc gamma RIIIa (CD16): differential ligand binding. *J. Immunol.* **159**:3849–3857.
26. Miller, K.L., Duchemin, A.M., and Anderson, C.L. 1996. A novel role for the Fc receptor gamma subunit: enhancement of Fc gamma R ligand affinity. *J. Exp. Med.* **183**:2227–2233.
27. Garman, S.C., Wurzburg, B.A., Tarchevskaya, S.S., Kinet, J.P., and Jardetzky, T.S. 2000. Structure of the Fc fragment of human IgE bound to its high-affinity receptor Fc epsilon RI alpha. *Nature.* **406**:259–266.
28. Kalesnikoff, J., et al. 2001. Monomeric IgE stimulates signaling pathways in mast cells that lead to cytokine production and cell survival. *Immunity.* **14**:801–811.
29. James, L.C., Roversi, P., and Tawfik, D.S. 2003. Antibody multispecificity mediated by conformational diversity. *Science.* **299**:1362–1367.
30. Kohno, M., Yamasaki, S., Tybulewicz, V.L., and Saito, T. 2005. Rapid and large amount of autocrine IL-3 production is responsible for mast cell survival by IgE in the absence of antigen. *Blood.* **105**:2059–2065.
31. Kitaura, J., et al. 2003. Evidence that IgE molecules mediate a spectrum of effects on mast cell survival and activation via aggregation of the Fc epsilon RI. *Proc. Natl. Acad. Sci. U. S. A.* **100**:12911–12916.
32. Schweitzer-Stenner, R., and Pecht, I. 2005. Death of a dogma or enforcing the artificial: monomeric IgE binding may initiate mast cell response by inducing its receptor aggregation. *J. Immunol.* **174**:4461–4464.
33. Bruhns, P., Fremont, S., and Daëron, M. 2005. Regulation of allergy by Fc receptors. *Curr. Opin. Immunol.* **17**:662–669.
34. Takhar, P., et al. 2007. Class switch recombination to IgE in the bronchial mucosa of atopic and non-atopic patients with asthma. *J. Allergy Clin. Immunol.* **119**:213–218.
35. Takhar, P., et al. 2005. Allergen drives class switching to IgE in the nasal mucosa in allergic rhinitis. *J. Immunol.* **174**:5024–5032.
36. Thomas, P.S., Yates, D.H., and Barnes, P.J. 1995. Tumor necrosis factor-alpha increases airway responsiveness and sputum neutrophilia in normal human subjects. *Am. J. Respir. Crit. Care Med.* **152**:76–80.
37. Lukacs, N.W., Strieter, R.M., Chensue, S.W., Widmer, M., and Kunkel, S.L. 1995. TNF-alpha mediates recruitment of neutrophils and eosinophils during airway inflammation. *J. Immunol.* **154**:5411–5417.
38. Amrani, Y., Chen, H., and Panettieri, R.A., Jr. 2000. Activation of tumor necrosis factor receptor 1 in airway smooth muscle: a potential pathway that modulates bronchial hyper-responsiveness in asthma? *Respir. Res.* **1**:49–53.
39. Berry, M.A., et al. 2006. Evidence of a role of tumor necrosis factor alpha in refractory asthma. *N. Engl. J. Med.* **354**:697–708.
40. Gould, H.J., and Sutton, B.J. 2008. IgE in allergy and asthma today. *Nat. Rev. Immunol.* **8**:205–217.
41. Andren, M., Johanneson, B., Alarcon-Riquelme, M.E., and Kleinau, S. 2005. IgG Fc receptor polymorphisms and association with autoimmune disease. *Eur. J. Immunol.* **35**:3020–3029.
42. Ioan-Facsinay, A., et al. 2002. Fc gamma RI (CD64) contributes substantially to severity of arthritis, hypersensitivity responses, and protection from bacterial infection. *Immunity.* **16**:391–402.
43. Dombrowicz, D., Flamand, V., Brigman, K.K., Koller, B.H., and Kinet, J.P. 1993. Abolition of anaphylaxis by targeted disruption of the high affinity immunoglobulin E receptor alpha chain gene. *Cell.* **75**:969–976.
44. Yu, P., Kosco-Vilbois, M., Richards, M., Kohler, G., and Lamers, M.C. 1994. Negative feedback regulation of IgE synthesis by murine CD23. *Nature.* **369**:753–756.
45. Hamada, K., et al. 2003. Allergen-independent maternal transmission of asthma susceptibility. *J. Immunol.* **170**:1683–1689.
46. Bruhns, P., Marchetti, P., Fridman, W.H., Vivier, E., and Daëron, M. 1999. Differential roles of N- and C-terminal immunoreceptor tyrosine-based inhibition motifs during inhibition of cell activation by killer cell inhibitory receptors. *J. Immunol.* **162**:3168–3175.
47. Latour, S., Bonnerot, C., Fridman, W.H., and Daëron, M. 1992. Induction of tumor necrosis factor-alpha production by mast cells via Fc gamma R. Role of the Fc gamma RIII gamma subunit. *J. Immunol.* **149**:2155–2162.